A Study entitled
Research on Orbital Plasma-Electrodynamics (ROPE)

Contract No. NAS8-37107

Progress Report
Period of Performance: March 27, 1994 - June 29, 1994

by

S. T. Wu
and
K. Wright
Center for Space Plasma and Aeronomic Research
The University of Alabama in Huntsville
Huntsville, AL 35899

for

National Aeronautics and Space Adminstration
George C. Marshall Space Flight Cetner
Marshall Space Flight Cetner, AL 35812

August 1994

The development of current collection model has been completed. The detailed description of this model has been presented and an article has been submitted to the J. of Geophysical Research for publication. The manuscript entitled "Three-Dimensional Current Collection Modesl fo a Highly Positive Potential Satellite in Space" is enclosed with this report.

Three Dimensional Current Collection Models of a Highly Positive Potential Satellite in Space

A. Shiah, S. T. Wu

Center for Space Plasma and Aeronomic Research

Univ. of Alabama in Huntsville

Huntsville, AL 35899

N. H. Stone

Space Science Laboratory

NASA/Marshall Space Flight Center

Huntsville, AL 35812

and

K. S. Hwang

Grumman Space Station Integration Division

620 Discovery, Huntsville, AL 35806

Abstract

Since the early development of probe theory by Langmuir and Blodgett [1924], the problem of current collection by a charged spherically or cylindrically symmetric body has been investigated by a number of authors (e.g. Parker and Murphy, 1967; Linson, 1969; Laframboise and Rubinstein, 1982). This paper overviews the development of a fully three-dimensional particle simulation code which can be used to understand the physics of current collection in three dimensions and can be used to analyze data resulting from the future TSS (Tethered Satellite System) mission.

According to the configuration of TSS, we have construct two types of particle simulation models, a simple-particle simulation (SIPS) model and a super-particle simulation (SUPS) model, to study the electron transient response and its asymp-

totic behavior around a three dimensional, highly biased satellite. The potential distribution surrounding the satellite is determined by solving Laplace's equation in the SIPS model and by solving Poisson's equation in the SUPS model. Thus, the potential distribution in space is independent of the density distribution of the particles in the SIPS model but it **does** depend on the density distribution of the particles in the SUPS model. The evolution of the potential distribution in the SUPS model can be described as follows: (1) The potential distribution is spherically symmetric in the beginning, (2) A spheroidal potential distribution occurs in the region closest to the high potential satellite, (3) A dumbbell-shaped potential distribution eventually forms with areas of high potential in the polar regions. When the spherical satellite is charged to a highly positive potential and immersed in a plasma with a uniform magnetic field, the formation of an electron torus in the equatorial plane (the plane is perpendicular to the magnetic field) and elongation of the torus along the magnetic field are found in both the SIPS and the SUPS models but the shape of the torus is different. The areas of high potential that exist in the polar regions in the SUPS model exaggerates the elongation of the electron torus along the magnetic field. The current collected by the satellite for different magnetic field strengths are investigated in both the SIPS and SUPS models. Due to the nonlinear effects present in the SUPS model, the oscillating phenomenon of the current collection curve during the first 10 plasma periods can be seen (this does **not** appear in the SIPS model). From the parametric studies, we find that the oscillating phenomenon of the current collection curve occurs only when the magnetic field strength is less than 0.2 *gauss* for the present model in this paper.

1. Introduction

The Tethered Satellite System (TSS) is one of the numerous applications of current collection by conducting bodies in a space plasma environment. Utilization of TSS could enable us to understand the fundamental characteristics of space plasma in the near earth environment and technologically test the possibility of current collection in space. For an eastward-moving satellite-tether-shuttle system, the satellite will be charged positively while the shuttle will be charged negatively with respect to the ambient ionospheric plasma. A current circuit can be closed by using the highly positive potential satellite to collect electrons from space and two electron guns located in the shuttle cargo bay to eject collected electrons back into space. When the satellite is biased to a highly positive potential, the particles surrounding the satellite are influenced by the combined effects of the electric and magnetic fields. In order to understand the physical phenomena of this configuration, the study of current collection by a highly biased potential satellite becomes important.

Early studies of a highly charged sphere in a space plasma can be classified into qualitative and quantitative analyses. The qualitative behaviors of an electron torus in the equatorial plane (perpendicular to the magnetic field line) surrounding a highly charged sphere were described by the laboratory observations such as Quinn and Chang [1966], Quinn and Fiorito [1967], Antoniades et al. [1990], Alport et al. [1990], and Greaves et al. [1990]. The quantitative analyses of possible current collected by a charged sphere in a space plasma were done by Parker and Murphy [1967], Linson [1969], and Rubinstein and Laframboise [1982]. Parker and Murphy [1967] used the conservation of a single particle's canonical angular momentum to evaluate the maximum possible current collected by a spherical probe in a uniform magnetic field neglecting particle thermal motion and turbulent effects. Linson [1969] introduced a parameter q_c representing the turbulent effect (q_c is determined

from experiments) to modified the Parker-Murphy model and presented a constant density cylindrical shielding model. Taking into account the contribution from those particles with encircling orbits, Rubinstein and Laframboise [1982] used kinetic theory to develop an analytical form estimating the upper bound current collected by a spherical probe. However, the previous quantitative studies are concerned with the estimation of steady state current collection by a high potential sphere (the comparison between those previous quantitative studies and our numerical results will be discussed in section 3 of this paper) while the transient response of electron behavior and the characteristic of instantaneous current collection curve have not been discussed.

The study of current collection at highly positive electrode voltages has recently become more prominent due to possible applications in the design of high-voltage power systems by using TSS. In an effort to investigate the physics of a highly biased potential satellite expected in the shuttle electrodynamic TSS-1 experiment, a number of numerical simulations have been performed. The numerical models used in the studies of TSS can be classified into fluid model (e.g. Ma and Schunk [1989] and Sheldon [1994]) and particle model (e.g. Hwang et al. [1990,1992], Vashi and Singh [1991], and Singh and Chaganti [1994]). In general, the fluid model describes the macroscopic behavior of the system while the particle model can better explain the microscopic behavior of each individual particles and their collective behavior. Ma and Schunk [1989] used a time-dependent fluid model to simulate the initial response of the particles around the highly biased potential sphere and found that an electron torus initially existed in the equatorial plane and eventually elongated along the magnetic field line. Sheldon [1994] used a steady state fluid model to study the electron current distribution and the angle of incidence of those collected electrons on the spherical satellite surface. To better understand the electron trajectory around the high potential satellite, Hwang et al. [1990]

utilized a two dimensional particle code to examine the electron trajectory in a static TSS-1 model. In their model, they indicated that electrons were trapped and the satellite was shielded when the magnetic field strength was greater than 0.35 *gauss*. This magnetic shielding is because of the $\vec{E} \times \vec{B}$ drift effect. Vashi and Singh [1991] used a $2\frac{1}{2}$ dimensional PIC (Particle in Cell) code to simulate the steady state current collection by a long conducting cylinder in a magnetized plasma. In their model, electrons are injected on the boundary of a prescribed high potential region and the initial space charge effect is neglected (i.e. assume the calculation region is initially a vacuum). Based on their previous investigations, Singh and Chaganti [1994] further studied the energy distribution of the particles on the satellite surface. They also found that the degree of current collection is dependent on the size of their prescribed high potential region.

In order to study the evolution of the electron distribution surrounding a highly positive potential satellite, Shiah et al. [1991] developed a three dimensional particle code. Instead of assuming that the initial calculation region is a vacuum, they initially put a finite number of Maxwellian electrons in the high potential region to study the time-dependent electron response. From their numerical results, an electron torus surrounded the high voltage satellite in the equatorial plane and oscillated between the satellite surface and plasma sheath. Hwang et al. [1992] also realized that the oscillation of the electron torus is a transient phenomenon. For longer run times, the electron torus will gradually elongate along the magnetic field line and finally become an "hour glass" distribution. This "hour glass" distribution is consistent with the "magnetic bottle" described by Parker and Murphy [1967] and the constant density cylindrical shielding model presented by Linson [1969]. The electron torus phenomena seen in numerical simulations (Shiah et al. [1991] and Hwang et al. [1992]) are also consistent with the earlier fluid model by Ma and Schunk [1989] and experimental observations by Quinn and Chang [1966], Quinn

and Fiorito [1967], Antoniades et al. [1990], Alport et al. [1990], and Greaves et al. [1990].

In the previous numerical simulations of TSS (e.g. Ma and Schunk [1989], Vashi and Singh [1991], Singh and Chaganti [1994], and Sheldon [1994]), the current collection models are either spherical or cylindrical symmetry without discussing the effect of ion's motion on electron distribution and the characteristic of instantaneous current collection in TSS. In order to see the effect of ion's motion on the transient response of TSS, this paper presents the simple-particle simulation (SIPS) and the super-particle simulation (SUPS) models. The SIPS model treats each simulation particle as one physical particle and the potential distribution in space is independent of the density distribution of the particles. As to the SUPS model, each simulation particle represents the center of mass of a particle cloud and the potential distribution in space is dependent on the density distribution of the particles. To the best of our knowledge, most of the previous current collection models use an approximation formula to describe the potential distribution around the high potential body (e.g. Parker and Murphy [1967], Linson [1969], Singh and Chaganti [1994]) while the space charge effect on the potential distribution and current collection have not been discussed. The SUPS model in this paper will take into account the space charge effect (a contribution from the ions and electrons) on the particle and potential distributions and the current collection. According to a realistic configuration of TSS mission, the physical model described in this paper includes a spherical satellite body, a cylindrical boom, and a spherical instrument (see figure 1). When the spherical satellite body is charged to highly positive potential, the electrons surrounding the satellite experience the electric and geomagnetic fields. To know the coupling effect of the electric and magnetic fields in three dimensions, the three dimensional electron trajectories are discussed in section 3 of this paper. Since the satellite velocity is much smaller than the electron thermal velocity, the

effect of the moving satellite is neglected for the present study. The basic theory and numerical method are described in Section 2 while the numerical results of the SIPS and the SUPS models are discussed in Section 3. The concluding remarks of this paper are given in Section 4.

2. Theory

In agreement with the actual TSS configuration, the model adopted in this paper assumes that a 40 cm diameter spherical instrument is attached to the 1.6 m diameter spherical satellite body by a 3 cm radius, 80 cm long cylindrical boom (see figure 1). The spherical satellite body is fixed at 500 V, the cylindrical boom floats at the local potential, and the spherical instrument can float at the local potential or be charged to a constant potential. The governing equations of this model now follow,

(a) Governing Equations:

The potential distribution in space is the first interesting thing to know in this paper. Instead of using the approximation formulas as the previous current collection models (e.g. Parker and Murphy [1967], Linson [1969], and Singh and Chaganti [1994]), the potential distribution in space is given by solving Laplace's equation in the SIPS model and by solving Poisson's equation in the SUPS model.

$$\text{for SIPS model: } \nabla^2\phi = 0 \tag{1.1}$$

$$\text{for SUPS model: } \nabla^2\phi = -4\pi\rho = 4\pi e(n_e - n_i) \tag{1.2}$$

where ρ is the plasma charge density, n_e is the electron density , n_i is the ion density, and ϕ is the space potential. Combining eqn (1.1) for the SIPS model (or eqn (1.2) for the SUPS model) with the following equation

$$\vec{E} = -\nabla\phi, \tag{2}$$

allows the potential and electric field in space to be determined.

The equations of motion for electrons and ions in the presence of magnetic and electric fields are

$$m_e \frac{d\vec{v}_e}{dt} = q_e\left(\vec{E} + \frac{\vec{v}_e \times \vec{B}}{c}\right) \tag{3}$$

$$m_i \frac{d\vec{v}_i}{dt} = q_i\left(\vec{E} + \frac{\vec{v}_i \times \vec{B}}{c}\right) \tag{4}$$

where $\vec{E}$ is calculated from equation (2) and $\vec{B}$ is the given magnetic field. The increment of particle positions can be obtained by

$$d\vec{r}_e = \vec{v}_e dt \tag{5}$$

$$d\vec{r}_i = \vec{v}_i dt \tag{6}$$

From equations (1) through (6), each individual particle trajectory is determined.

(b) Numerical Scheme:

In the simulation, the governing equations are solved in spherical coordinates and the grid points are allowed to cluster in an exponential fashion in the region of the boom and the instrument to reduce code memory and increase both the efficiency and accuracy.

In spherical coordinates, equations (1) and (2) can be expressed as follows (Ref. 3)

$$\frac{1}{r^2 sin\varphi}\left[\frac{\partial}{\partial r}\left(r^2 sin\varphi \frac{\partial\phi}{\partial r}\right) + \frac{\partial}{\partial\theta}\left(\frac{1}{sin\varphi}\frac{\partial\phi}{\partial r}\right) + \frac{\partial}{\partial\varphi}\left(sin\varphi\frac{\partial\phi}{\partial\varphi}\right)\right] = 4\pi e(n_e - n_i) \tag{7}$$

$$\vec{E} = -\frac{\partial \phi}{\partial r}\hat{r} - \frac{1}{r sin\varphi}\frac{\partial \phi}{\partial \theta}\hat{\theta} - \frac{1}{r}\frac{\partial \phi}{\partial \varphi}\hat{\varphi} \tag{8}$$

where r is in the radial direction, θ is in the azimuthal direction, and φ is in the direction from south pole to north pole.

The seven-point finite difference form of equation (7) can be expressed as

$$a_e\phi_{i+1,j,k} + a_w\phi_{i-1,j,k} + a_n\phi_{i,j+1,k} + a_s\phi_{i,j-1,k} + a_t\phi_{i,j,k+1} + a_b\phi_{i,j,k-1} - a_p\phi_{i,j,k} = 4\pi e(n_e - n_i)_{i,j,k} \tag{9}$$

Equation (9) can be written in matrix form as

$$M\Phi = F \tag{10}$$

where M is the coefficient matrix, Φ is the potential matrix and F is the charge density matrix. A powerful iterative method by Vinsome [1976] is chosen to solve eqn (10) in this paper.

The electric field is obtained by substituting the potential matrix solved in eqn (10) back into eqn (8). Substituting this electric field into the equations of motion (equations (3) and (4)) allows particle trajectories to be obtained by advancing the particle velocities and positions according to eqns (3) through (6). If initial particle positions and velocities are given, the new particle positions can be found. From these new particle positions, new density distributions of the particles can be obtained. In this paper, the SIPS model does not feed back the density distribution of the particles but the SUPS model will substitute the new density distributions back into Poisson's equation to close the iteration loop.

3. Results and Discussions

In the present three dimensional model, the spherical satellite body is charged to 500 V, the cylindrical boom is biased to local potential, and the spherical instrument can be charged to either local potential or a constant potential. To solve

this kind of satellite-plasma interaction problem, the only physical boundary is the surface of the satellite. However, for the simulation, an artificial zero potential boundary is required. To assure that the artificial boundary does not alter the actual physical situation, this boundary needs to be put well within the unperturbed plasma. For a conservative estimation, this zero potential boundary is chosen at 420 cm from the center of the spherical satellite body. The chosen zero potential boundary is much larger than the plasma sheath calculated by the Modified Child-Langmuir Law (Ref. 10).

In order to study the physics of this three dimensional current collection model, the simple-particle simulation (SIPS) and the super-particle simulation (SUPS) models are presented in this section. The comparison of initial potential distributions, when the spherical instrument is charged to a constant potential or allowed to float at the local potential, can be seen in figure 2. Figures 2.(a) and 2.(c) are the contour plots of the potential distribution on the Y-Z plane and figures 2.(b) and 2.(d) are the potential curves plotted along the boom direction (Y-axis). For the case of floating instrument potential, the potential drops from 500 V on the satellite surface to zero potential on the outer boundary with 420 cm radius (see figures 2.(a) and 2.(b)). The potential disturbance surrounding the instrument can be seen in figures 2.(c) and 2.(d) when the instrument potential is fixed at -100 V. In this case, the negative potential barrier near the instrument can exclude the surrounding electrons and disturb current collection. In order to reduce the disturbance of instrument potential on current collection, the instrument potential will be allowed to float at the local potential in our present studies. In the following sections, we will concentrate on the investigations of initial response for the electron distribution and current collection in both SIPS and SUPS models.

3.1 Simple-Particle Simulation (SIPS) Model

When the boundary conditions of Poisson's equation are given, the only factor that can influence the potential distribution is the density distribution of particles. In general, the effect of the density distribution can be neglected if the satellite potential is high and the absolute value of net space charge density is relatively low. The criterion for neglecting the density distribution is not the main purpose of this paper so that we will leave this topic to future studies. In our SIPS model, the initial and boundary conditions are as follows: There are 10,000 electrons and ions with Maxwellian velocity distributions uniformly located in the region between the satellite surface and the spherical zero potential boundary (see figure 3.(a)). The electron and ion temperature is 0.1 eV and the magnetic field is 0.4 $gauss$ along the Z-axis. The spherical satellite is charged to 500 V while the boom and the spherical instrument float at the local potential. To account for the effect of the particles coming from the plasma reservoir, particles are injected inward from the zero potential boundary at each calculation time step. The particle injection rate is determined by the assumption that the electric field will not influence the particles located outside the zero potential boundary. Therefore, the only cause for particles to strike the zero potential boundary is their thermal motion.

Since the electron thermal velocity is much faster than the ion thermal velocity, we are more interested in the initial response of the electrons. As the satellite potential is turned on, electrons experience the electric and geomagnetic fields. The three dimensional electron trajectories are investigated to determine the coupling effect of the electric and magnetic fields. According to the Parker and Murphy model, an electron will not be collected by the high potential satellite if it is originally located outside the critical radius r_0. The critical radius can be written as

$$r_0 = a\left[1 + \left(\frac{8|e\phi_s|}{m\omega_c^2 a^2}\right)^{\frac{1}{2}}\right]^{\frac{1}{2}}, \tag{11}$$

where ϕ_s is the satellite potential, a is the satellite radius, ω_c is the electron cyclotron frequency, e is the electron charge, and m represents the electron mass. For a 500

V spherical satellite with 80 cm radius located in the plasma with a 0.4 $gauss$ magnetic field strength in the positive Z direction, the critical radius calculated from equation (11) is equal to 191.18 cm.

To verify the Parker and Murphy theory by our SIPS model, the three dimensional trajectories of electrons with their initial positions located both inside and outside the critical radius are presented in figures 3 and 4. In figure 3, we place a 0.1 eV electron outside the critical radius at point A (i.e. the position is $x = 0.0$ cm, $y = 195$ cm, and $z = 500$ cm in the cartesian coordinates). Figure 3.(a) is the electron trajectory viewed in three dimensions and figure 3.(b) is the top view of the electron trajectory. When the electron is outside the zero potential boundary (from point A to point B in figure 3.(a)), the electron gyrates along the magnetic field line and its gyroradius is on the order of 1 cm. As long as the electron enters into the high potential region, the electron experiences the coupling effect of the electric and magnetic fields. In our model, the electric field is always in the positive radial direction (coming out the satellite surface) and the magnetic field is in the positive Z direction, thus, the $\vec{E} \times \vec{B}$ drift force is in the clockwise direction (from the top view). The electric force causes the electron to move from the northern hemisphere down to the southern hemisphere and from the southern hemisphere up to the northern hemisphere (see figure 3.(a)). The top view of the electron trajectory (see figure 3.(b)) shows that the clockwise electron motion is due to the $\vec{E} \times \vec{B}$ drift force and the counterclockwise gyration motion is because of the effect of the magnetic field. Figure 3.(b) also shows that the electron trajectory is confined inside the "magnetic bottle" described by Parker and Murphy [1967] and the satellite is magnetically shielded from the electron trajectory.

In figure 4, an electron with the same thermal velocity as figure 3 is located inside the critical radius at point A (i.e. the position is $x = 0.0$ cm, $y = 170$ cm, and $z = 500$ cm in the cartesian coordinates). The three dimensional electron

trajectory in figure 4.(a) shows that the coupling effect of the electric and magnetic field causes the electron to gyrate around the satellite. The $\vec{E} \times \vec{B}$ drift force moves the electron in the clockwise direction and the electron gyration motion is in the counterclockwise direction (see figure 4.(b)). Finally, the electron will be collected by the satellite (see figure 4.(b) point C). From the parametric studies, we found that the criterion to determine whether the electron will be collected by the satellite is not strictly defined by the critical radius described by equation (11). The difference results from neglecting electron thermal motion and having the different prescribed potential distribution in the Parker and Murphy model. To test the effect of magnetic field strength on electron trajectories, the magnetic field strength (0.4 *gauss* in figure 3) is increased to 0.5 *gauss* in figure 5. Comparing figures 5 and 3.(b) shows that the satellite shielded zone is increased with increasing magnetic field strength.

The evolution of the electron distribution can be seen in figure 6. From figures 6.(a) through 6.(c), a strong electron torus embedded in a tenuous electron cloud is gradually formed in the equatorial plane. When the calculation time is equal to 4.3 plasma periods (see figure 6.(d)), the tenuous electron cloud has disappeared and the strong electron torus has elongated along the magnetic field line. The formation of the electron torus in the equatorial plane and its elongation along the magnetic field line are similar to the early experimental observations by Quinn and Chang [1966], Quinn and Fiorito [1967], Antoniades, et al. [1990], Alport et al., [1990], and Greaves et al., [1990]. The trapping of electrons in the equatorial plane (see figure 6.(d)) is also consistent with the "magnetic bottle" described by Parker and Murphy [1967]. Although the phenomenon of an electron torus surrounding a highly charged sphere has discovered by previous observations and reported in the fluid model by Ma and Schunk [1989] and Sheldon [1994], the results simulated by our three dimensional particle code can better describe the relationship between

the formation of the electron torus and "magnetic bottle" described by Parker and Murphy [1967] in TSS. Since the characteristics of the current-voltage curve for a charged sphere have been studied by previous current collection models, this paper will concentrate on the investigation of the instantaneous current collection curve which has not been presented in previous studies.

During the first Tethered Satellite System (TSS-1) mission, the system was operated in the ionosphere with the plasma density in the range of $10^5\ cm^{-3}$ to $10^6\ cm^{-3}$ which corresponds to 10^{13} total particles in the present model. Due to the limitation of computer memory and calculation time, it is impossible to use so many simulation particles in our calculation. In the SIPS model, a factor described by Singh and Chaganti [1994] can be used to scale up the simulation particles to the level of the physical particles. This scale up factor f_c can be written as

$$f_c = \frac{n_0 V_{tot}}{N_{tot}} \tag{12}$$

where n_0 is the ambient plasma density, V_{tot} is the volume of calculation region, and N_{tot} is the number of particles in the simulation. Thus, the current collected by the satellite can be estimated as

$$I = f_c \frac{\Delta N_c e}{\Delta t} \tag{13}$$

where ΔN_c is the number of the collected electrons per time step, e is the electron charge, and Δt is the magnitude of each numerical calculation time step. When the satellite potential is turned on, the electrons experience a three dimensional Lorentz force. The electric force causes electrons to move radially toward the satellite surface while the $\vec{E} \times \vec{B}$ drift force causes electrons to gyrate in the azimuthal direction. The influence of the magnetic field strength on the current collection curve can be seen in figure 7. In figure 7.(a), the collected current reaches a peak value of 2.4 *amp* at 1.4 plasma periods and decreases to a small value after 4.3 plasma periods.

If we look at the electron distribution, it is clear that the current curve drops to a small value at 4.3 plasma periods is due to the strong electron torus formed in the equatorial plane at that time. Furthermore, the second pulse seen in figure 7.(a) is because of the changing of the electron distribution from a strong electron torus to a cylindrical shielding zone at this time. After 10 plasma periods, the instantaneous current will reach a quasi-steady state value on the order of 10^{-2} A.

As the magnetic field strength is increased, the time needed to reach the peak current as well as the magnitude of the peak current are decreased (i.e. it takes 0.9 plasma periods to reach 1.6 *amp* in figure 7.(b) and 0.3 plasma periods to reach 1.0 *amp* in figure 7.(c)). This phenomenon can be explained as follows: When the magnetic field strength is increased, the increasing effect of the $\vec{E} \times \vec{B}$ drift force tends to move electrons in the azimuthal direction instead of the radial direction. This increasing azimuthal motion can cause electrons to stay in the high potential region longer than before and reduce the current collection rate during the first 10 plasma periods. From the previous studies of the electron distribution, it was seen that the electron torus initially forms in the equatorial plane and eventually elongates along the magnetic field line. By comparing the electron distribution with the current collection curve, one sees that the formation and elongation of the electron torus will be accomplished in less than 10 plasma periods. After 10 plasma periods, most of the gyrating electrons will be collected by the satellite so that the collected current approaches a quasi-steady state value.

For a sphere with radius a in a plasma, the random current I_R caused by the electron thermal motion can be expressed as

$$I_R = 4\pi a^2 e n_0 \left(\frac{kT}{2\pi m_e}\right)^{\frac{1}{2}} \tag{14}$$

where k is Boltzmann's constant, and T and n_0 are the temperature and ambient number density of the electrons. On the basis of this definition of random current

I_R, a spherical body with 80 cm radius can collect 6.8 mA random current from an ambient plasma with 0.1 eV temperature and 10^5 cm^{-3} density. When this spherical body is charged to a positive potential and immersed in a plasma with a magnetic field, the electric field tends to increase the current collection while the $\vec{E} \times \vec{B}$ drift force tends to decrease the current collected by the high potential body. Whether the current collected by the charged body should be larger than the random current depends on the potential on the charged body and the magnetic field strength. According to our physical model, the estimates of current collection from Parker and Murphy [1967] and Rubinstein and Laframboise [1982] are on the order of 0.02 A. In figure 7, the quasi-steady state current after 10 plasma periods is on the order of 0.02 to 0.04 A which is larger than the random current and similar to the estimates from Parker and Murphy [1967] and Rubinstein and Laframboise [1982].

3.2 Super-Particle Simulation (SUPS) Model

In the previous discussions, the simple-particle simulation (SIPS) model is only valid for the highly charged potential satellite in a relatively low density plasma and it treats each simulation particle as one physical particle. In the super-particle simulation (SUPS) model, particles are regarded as finite-sized clouds of electrons or ions, the position of the superparticles being the center of mass of the clouds and their velocities being the mean velocities of the electrons or ions. In order to use the limited simulation particles to study millions of physical particles, the scale up factor described by equation (12) can be used to magnify the charge and mass of the simulation particles to the level of the particle clouds. Due to the increasing charge and mass of the simulation particles, the time-dependent density distribution of the particles becomes important and can not be ignored in the calculation. Hence, a self-consistent iteration loop described in section 2 is required to update

the superparticles information at each iteration cycle. In order to assign the superparticle's information to the grid points, a suitable particle assignment function is required. The necessary properties of a particle assignment function are that the assignment should satisfy the long range constraint and the smoothness constraint. The long range constraint means that the assignment should be over a number of grid points far from the source charge and the smoothness constraint means that the assignment should vary smoothly with the location of the particles. To accomplish these constraints, the *sinc* function described by Hockney and Eastwood [1988] is chosen as the superparticle assignment function in this study. In this section, we will discuss one-component (i.e. only electrons are considered) and two-component (i.e. electrons and ions are considered) cases. The one-component case does not represent a real situation in space. The reason for showing it is to emphasize the importance of ion motion in the SUPS model.

As we mentioned in the SIPS model, when the boundary conditions are given, the only factor that can influence the potential distribution is the source term in Poisson's equation (i.e. $4\pi e(n_i - n_e)$ in equation (1.2)). The negative source term tends to decrease the space potential while the positive source term tends to increase the space potential. For the one-component case, we only include electrons in the calculation and ignore the existence of the ions. When the ions are not considered, the source term in Poisson's equation becomes negative and will drop the potential to a negative value. Figure 8.(b) shows that, in this case, the negative potential region appears in most of the calculation domain at 0.86 plasma periods even if the satellite potential is fixed at 500 V positive.

For the two-component case, electrons and ions are both considered in the calculation. The contour plot of the potential distribution in Y-Z plane and the potential curve along the boom direction (Y-axis) at 0.86 plasma periods are plotted in figures 8.(c) and 8.(d) (electrons and ions **are** considered). Due to the existence of

the ions, the negative potential region in figures 8.(a) and 8.(b) (produced when ions are **not** considered) will disappear. It shows that the spheroid potential distribution occurs in the region close to the satellite (see figure 8.(c)) and the potential smoothly decays from 500 V on the satellite surface ($R = 80\ cm$) to zero at the zero potential boundary ($R = 420\ cm$) (see figure 8.(d)). From the previous discussion and the comparison of figures 8.(a).(b) and 8.(c).(d), it can be concluded that the existence of the ions **does** play an important role (i.e. ions neutralize the negative space charge) in the real physical problem.

To examine the effect of the ion population on electron behavior in the SUPS model, the evolution of electron transient response is shown in figure 9. In the SUPS model (see figure 9), the formation of the electron cloud and the electron torus are similar to the SIPS model (see figure 6). As the calculation time increases, the electron cloud surrounding the satellite (see figure 9.(b)) gradually becomes a strong electron torus in the equatorial plane (see figure 9.(c)) and eventually elongates along the magnetic field line (see figure 9.(d)). As the electron torus forms in the equatorial plane, the high potential areas gradually develop in the polar regions (see figures 10 and 11). Comparing figure 9.(d) with figure 6.(d), one sees that the high potential areas in the polar regions will attract the electrons from the torus and cause the torus to stretch along the magnetic field line faster than it would in the SIPS model. From the numerical results, the evolution of the potential distribution can be understood as the potential changing from a spheroidal distribution with the major axis along the magnetic field line (see figure 10) to a dumbbell distribution with two high potential areas in the polar regions (see figure 11). Owing to the existence of these two high potential areas, the ions will be gradually excluded from these areas as the calculation time increases (see figure 12). The phenomenon of excluding ions along the magnetic field line can cause the zero potential boundary to extend along the magnetic field line. Therefore, the chosen spherical zero potential

boundary needs to be modified in future simulation studies of the steady state.

In addition to the previous investigations of the particle and potential distributions, we are further interested in the study of quasi-steady state current collected by the satellite in the SUPS model. The current collected by the satellite is shown in figure 13 for different magnetic field strengths. It should be noted that the peak value of the current decreases with increasing magnetic field strength. After 10 plasma periods, the current collection curve will reach a quasi-steady state value on the order of 0.1 *amp* which is larger than the quasi-steady state current predicted in the SIPS model (0.02 to 0.04 A in figure 7). The difference of quasi-steady state current between SIPS and SUPS models could be due to the buildup of high potential regions in the SUPS model that are not included in the SIPS model. Another interesting thing is the characteristic of the current collection curve before 10 plasma periods when the magnetic field strength is 0.2 *gauss* (see figure 13.(a)). In order to determine why the current collection curve has several peaks in this region, we present four electron distributions at the peaks and valleys of the current collection curve. The electron distributions in figures 14.(a), (b), (c), and (d) are at the same times as positions (1), (2), (3), and (4) in figure 13.(a). When the satellite is shielded by the electron torus (see figures 14.(a) and 14.(c)), the current collection curve drops down to a minimum (positions (1) and (3) in figure 13.(a)). On the contrary, when the shielding torus collapses (see figures 14.(b) and 14.(d)), the current collection curve climbs to a peak (positions (2) and (4) in figure 13.(a)). According to our parametric studies, this character of the current collection curve before 10 plasma periods happens when the magnetic field strength is lower than 0.2 *gauss*. If we combine equations (3) and (5) together, the electron position can be described by

$$m_e \frac{d^2\vec{r}_e}{dt^2} + \frac{q_e}{c}\vec{B} \times \frac{d\vec{r}_e}{dt} - q_e\vec{E}(r_e,t) = 0 \qquad (15)$$

where $\vec{E}(r_e,t)$ is a function of time and particle position. The second term of

equation (15) tends to change the direction of the electron motion and keeps the electrons from moving toward the satellite. The third term of equation (15) is a time-dependent nonlinear term which tends to move electrons toward high potential regions. If we compare equation (15) with a 1-D spring system, the second term of equation (15) is similar to the damping force and the third term of equation (15) resembles the combined effect of the spring force and a time-dependent external force. When the damping force is lower than a critical value, the system will undergo vibration. Due to the coupling effect of the second and third terms in equation (15), the current collection curve may oscillate for a while when the magnetic field strength is lower than some specific value (e.g. 0.2 *gauss* for a 500 V potential satellite in our model). In a strict sense, equation (15) is a three dimensional equation and the magnetic field does not dissipate energy so that the electron behavior is not the same as a 1-D spring system. If we compare figures 13.(a) with 7.(a), one sees that the oscillating current curve does not occur in the SIPS model. This is another effect caused by ion motion in the SUPS model.

4. Concluding remarks

In this paper, we have developed a fully three dimensional self-consistent code with realistic geometry of TSS to study the current collection problem by using the simple-particle simulation (SIPS) and the super-particle simulation (SUPS) models. In general, the SIPS model treats each simulation particle as one physical particle and the effect of the density distribution of the particles can be neglected. As a result, the electric field is independent of the time in the SIPS model. On the other hand, the SUPS model regards each simulation particle as a finite-sized particle cloud (this can be defined as a superparticle). Due to the increased charge and mass of the superparticle, the effect of the density distribution of the particles becomes important, thus, the electric field is time-dependent in the SUPS model. When

the potential of the satellite is turned on in the plasma with a constant magnetic field, a strong electron torus embedded in a tenuous electron cloud will form in the equatorial plane as shown in both the SIPS and the SUPS models.

In the SIPS model, the tenuous electron cloud will disappear and the strong electron torus will gradually elongate along the magnetic field after a longer computer run time. Finally, the electron torus becomes an "hour glass" shielding zone which is similar to the "magnetic bottle" described by Parker and Murphy [1967]. According to the investigation of the three dimensional electron trajectory, the satellite is shielded from the electron trajectory if the initial position of the electron is located outside the critical radius described by Parker and Murphy [1967]. The shielding zone of the satellite is increased with increasing magnetic field strength. From the investigation of current collection by the satellite, we find that the peak value of the current collection curve decreases with increasing magnetic field strength and the current curve will reach a quasi-steady state value on the order of 10^{-2} A after 10 plasma periods.

In the SUPS model, ion motion will influence not only the electron distribution but also the current collected by the satellite. From our numerical results, the spheroid potential distribution around the satellite surface only exists during the early stage. After the formation of the electron torus in the equatorial plane, high potential areas will form in the polar regions as a result of the rapid evacuation of electrons along the field lines that terminates on the satellite. These high potential areas in the polar regions can attract the electrons from the electron torus in the equatorial plane, thus, the elongation of the electron torus along the magnetic field line in the SUPS model is faster than that in the SIPS model. In addition, the ions will be gradually excluded from the high potential areas in the polar regions. In fact, over much longer time, this region of positive space charge should propagate along the field lines away from the satellite at the ion acoustic speed. As a result

of the effect of ions in the SUPS model, the peak current in the SUPS model is less than that in the SIPS model but the quasi-steady state current in the SUPS model is larger than that in the SIPS model. The inclusion of ions also appears to cause the oscillations of the current collected by the satellite during the first 10 plasma periods. When the satellite is shielded from the electron torus, the collected current drops to a minimum. When the electron torus collapses by the electric force, the collected current increases to a peak value. This oscillating phenomenon only occurs when the magnetic field strength is lower than 0.2 *gauss* and disappears after 10 plasma periods in our model.

In summary, the transient response of the electron distribution and current collection have been investigated by using the SIPS and the SUPS models. The SIPS model is only valid for a highly biased potential satellite in a relatively low density plasma (i.e. the space charge effect is neglected) while the SUPS model can be used in the most general case (i.e. the space charge effect is included). From our previous numerical results, the best approach to investigate the effect of ion's motion on current collection is to use the SUPS model with the inclusion of ions. The three dimensional self-consistent particle code developed in this paper, including the density distribution effect and the interaction of three dimensional electric and magnetic fields, is essentially new and has a wide range of applications. Particularly, this code can be used to investigate the particle and potential distributions around three dimensional bodies and predict the collected electron current by the system. This is especially applicable to the reflight of the TSS experiment. In addition, there are several parameters (i.e. satellite potential, boom potential, magnetic field strength, instrument position, and instrument potential) that could be changed to study the current collection problem in different regions of parameter space. Furthermore, these models can be used to investigate several other topics of interest to the TSS mission (e.g. the wake effect due to the satellite motion, the distribution of

collected electron energy, and the position of the collected electrons on the satellite, boom or instrument surfaces). In the TSS-1 mission, the resolution of the instrument is on the order of 10^{-3} seconds, thus, the experimental measurements can not resolve the temporal effects discussed in this paper. The limitation of our model is that the short time step required in our simulation currently makes it impractical to model on timescales comparable to the resolution limit of the instrument on the TSS-1 satellite. If, at this short time, steady state conditions are reached, then it should apply. Otherwise, a much longer numerical simulation time is needed for the study of current collection problem in a steady state situation.

Acknowledgment

This work was supported by the National Aeronautics and Space Administration under contract NAS8-37107. The authors wish to thank Dr. G. R. Wilson for valuable discussions and suggestions.

References

1. Alfvén, H., *Cosmical Electrodynamics*, Oxford University Press, New York, 1953.
2. Alport, M. J., Antoniades, J. A., Boyd, D. A., Greaves, R. G., and Ellis, R. F., Electrical breakdown at low pressure in the presence of a weak magnetic field, *J. Geophys. Res., 95*, #A5, 6145-6153, 1990.
3. Anderson, D. A., Tannehill, J. C., and Pletcher, R. H., *Computational Fluid Mechanics and Heat Transfer*, Hemisphere, Washington, D. C., 1984.
4. Antoniades, J. A., Greaves, R. G., Boyd, D. A., and Ellis, R., Current collection by high voltage anodes in near ionospheric conditions, *NASA CP-3089*, 202-213, 1990.
5. Greaves, R. G., Boyd, D. A., Antoniades, J. A., and Ellis, R. F., Steady-state toroidal plasma around a spherical anode in a magnetic field, *Phys. Rev. Lett., 64*, #8, 886-889, 1990.
6. Hwang, K. S., Wu, S. T., Stone, N. H., and Wright, K. H. Jr., Current collection model on tether satellite system, *AIAA-90-0723, 28th Aerospace Sciences Meeting*, Reno, Nevada, Jan., 1990.
7. Hwang, K. S., Shiah, A., Wu, S. T., and Stone N. H., Three- dimensional current collection model, *AIAA 92-2988, AIAA 23nd Plasmadynamics & Lasers Conference*, Nashville, Tennessee, July, 1992.
8. Hockney, R. W. and Eastwood J. W., *Computer simulation using particles*, Institute of Physics Publishing, 1988.
9. Laframboise, J. G. and Rubinstein, J., Theory of a cylindrical probe in a collisionless magnetoplasma, *Phys. Fluids, 19*, #12, 1900-1908, 1976.
10. Langmuir and Blodgett, Currents limited by space charge between concentric spheres, *Phys. Rev., 23*, 49, 1924.

11. Linson, L. M., Current-voltage characteristics of an electron- emitting satellite in the ionosphere, *J. Geophys. Res.*, *74*, 2368-2375, 1969.

12. Ma, T. -Z. and Schunk, R. W., A fluid model of high voltage spheres in the ionosphere, *Planet. Space Sci.*, *37*, #1, 21-47, 1989.

13. Parker, L. W. and Murphy, B. L., Potential buildup on an electron-emitting ionospheric satellite, *J. Geophys. Res.*, *72*, 1631-1636, 1967.

14. Quinn, R. G. and Chang, C. C., Laboratory observations of a stable plasma trapped in a permanent dipolar magnetic field, *J. Geophys. Res.*, *71*, 253-262, 1966

15. Quinn, R. G. and Fiorito, R. B., Investigation of laboratory plasma instabilities in a dipole magnetic field, *J. Geophys. Res.*, *72*, 1611-1630, 1967.

16. Rubinstein, J. and Laframboise, J. G., Theory of a spherical probe in a collisionless magnetoplasma, *Phys. Fluids*, *25*, #7, 1174-1182, 1982.

17. Sheldon, J. W., High-voltage electron collection by a spherical satellite, *J. Geophys. Res.*, *99*, #A4, 6227-6232, 1994.

17. Shiah, A., Hwang, K. S., Wu, S. T., and Stone, N. H., Three dimensional time-dependent current collection model, *SM22A-11, AGU fall meeting*, San Francisco, California, Dec., 1991.

18. Singh N. and Chaganti V. S., Electron collection by a highly positive satellite in the ionosphere : Test particle simulation, *J. Geophys. Res.*, *99*, 469-478, 1994.

19. Störmer, C. *The Polar Aurora*, Oxford University Press, New York, 1955.

20. Vashi, B. I. and Singh, N., Current collection by a long conducting cylinder in a flowing magnetized plasma, *J. Spacecraft and Rocket, 28*, #5, 592-598, 1991.

21. Vinsome, P. K. W., ORTHOMIN, An iterative method for solving sparse sets of simultaneous linear equations, Paper *SPE 5729* presented at the SPE 1976 Numerical Simulation of Reservoir Performance Symposium, Feb., 1976.

Figure Captions

Fig. 1 The three dimensional current collection model. ($R_S = 80\ cm$ is the radius of the spherical satellite body, $R_I = 20\ cm$ is the radius of the spherical instrument, $L_B = 80\ cm$ is the length of the cylindrical boom, and $R_O = 420\ cm$ is the zero potential boundary)

Fig. 2 The effect of the instrument potential on the initial potential distribution: (a) the potential distribution on the Y-Z plane (instrument is floated to local potential). (b) the potential curve along the boom direction (instrument is floated to local potential). (c) the potential distribution on the Y-Z plane (instrument is biased to $-100\ V$). (d) the potential curve along the boom direction (instrument is biased to $-100\ V$).

Fig. 3 The electron originally located outside the critical radius at $x = 0.0\ cm$, $y = 195\ cm$, and $z = 500\ cm$ in cartesian coordinates. ($\phi_s = 500\ V$, $B = 0.4\ gauss$ in the positive Z direction). (a) the 3-D electron trajectory. (b) the top view of the electron trajectory.

Fig. 4 The electron originally located outside the critical radius at $x = 0.0\ cm$, $y = 170\ cm$, and $z = 500\ cm$ in cartesian coordinates. ($\phi_s = 500\ V$, $B = 0.4\ gauss$ in the positive Z direction). (a) the 3-D electron trajectory. (b) the top view of the electron trajectory.

Fig. 5 The top view of the electron trajectory. Electron originally located outside the critical radius at $x = 0.0\ cm$, $y = 195\ cm$, and $z = 500\ cm$ in cartesian coordinates. ($\phi_s = 500\ V$, $B = 0.5\ gauss$ in the positive Z direction).

Fig. 6 The evolution of the electron distribution in the SIPS model. ($\phi_s = 500\ V$, $B = 0.4\ gauss$ in the positive Z direction)

Fig. 7 The effect of the magnetic field strength on current collection in the SIPS model. The peak value of the current is decreased with the increasing magnetic field strength and the current reaches a quasi-steady state value on the order of 10^{-2} A after 10 plasma periods.

Fig. 8 The comparison of potential distribution around the satellite between one-component (ions are not considered) and two-component (electrons and ions are considered) cases in the SUPS model. (the calculation time is equal to 0.86 plasma periods).

Fig. 9 The evolution of the electron distribution in the SUPS model. ($\phi_s = 500$ V, $B = 0.4$ $gauss$ in the positive Z direction)

Fig. 10 The potential distribution around the satellite with the consideration of ion motion in the SUPS model (the calculation time is equal to 1.14 plasma periods). The spheroid potential distribution exists in the region close to the satellite body.

Fig. 11 The potential distribution around the satellite with the consideration of ion motion in the SUPS model (the calculation time is equal to 2.846 plasma periods). Due to the high population of ions in the polar regions, a high potential distribution can be built up in the north and south poles.

Fig. 12 The ion distribution in the SUPS model (the calculation time is equal to 22.768 plasma periods). Due to the existence of the high potential area in the polar regions, the ion density in the polar regions is lower than the equatorial region.

Fig. 13 The effect of the magnetic field strength on current collection in the SUPS model. The peak value of the current is lower than the SIPS model and the quasi-steady state current is on the order of 0.1 amp which is larger than the SIPS model.

Fig. 14 The evolution of the electron distribution in the SUPS model. The magnetic field is 0.2 *gauss* in the positive Z-direction. The electron distributions of (a), (b), (c), and (d) relate to positions (1), (2), (3), and (4) in figure 13.(a).

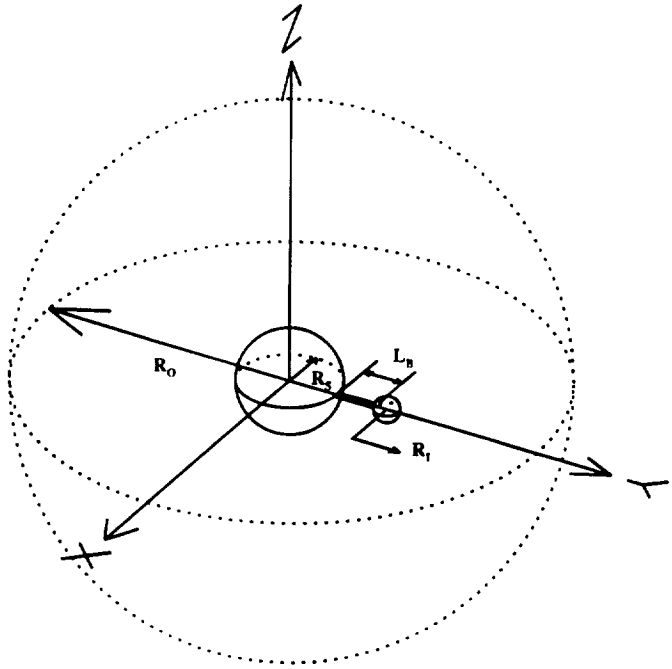

fig 1

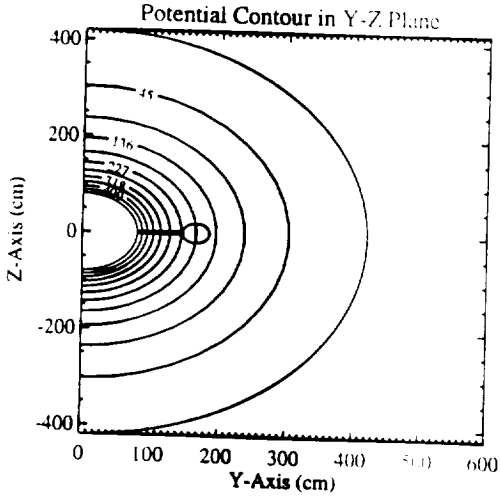
Potential Contour in Y-Z Plane
400
200
0
-200
-400
Z-Axis (cm)
0
100
200
300
400
500
600
Y-Axis (cm)

(a)

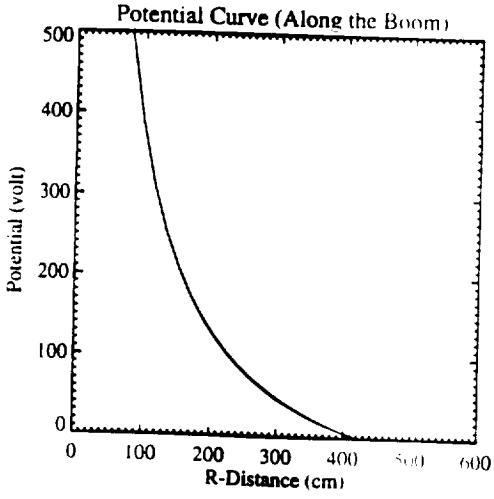
Potential Curve (Along the Boom)
500
400
300
200
100
0
Potential (volt)
0
100
200
300
400
500
600
R-Distance (cm)

(b)

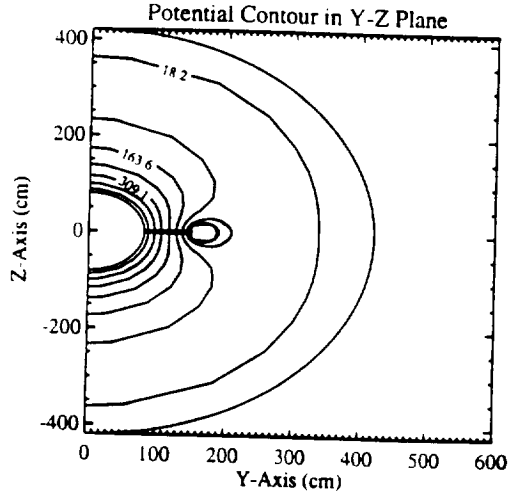
Potential Contour in Y-Z Plane
400
200
0
-200
-400
Z-Axis (cm)
182
1636
3091
0
100
200
300
400
500
600
Y-Axis (cm)

(c)

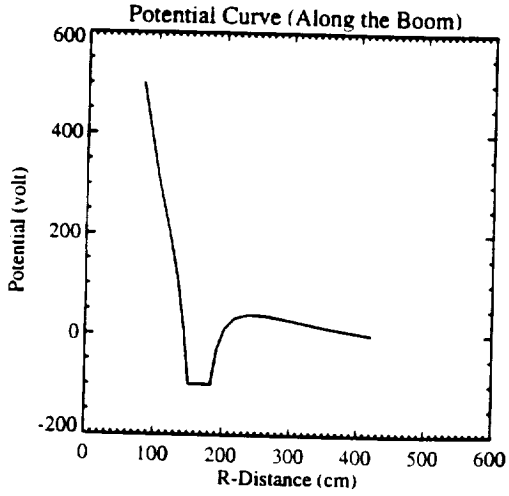
Potential Curve (Along the Boom)
600
400
200
0
-200
Potential (volt)
0
100
200
300
400
500
600
R-Distance (cm)

(d)

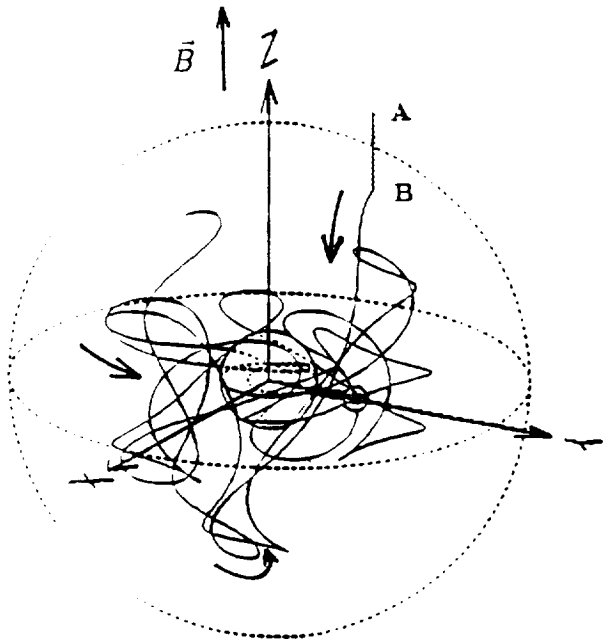

(a) 3-D view

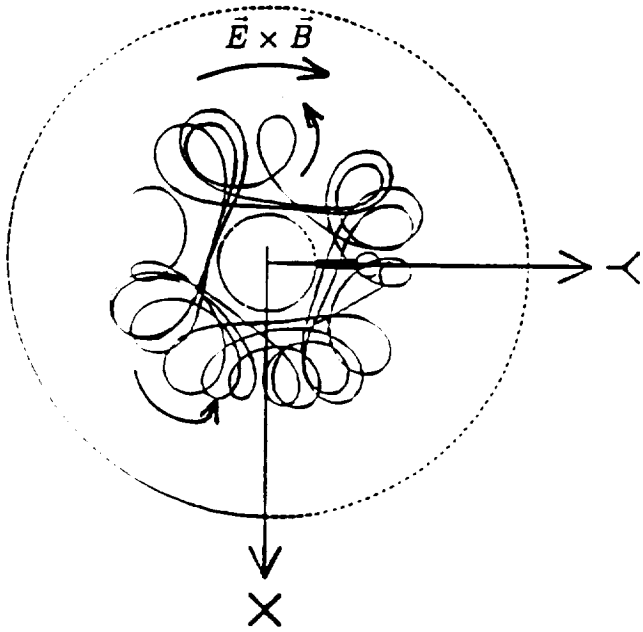

(b) Top view

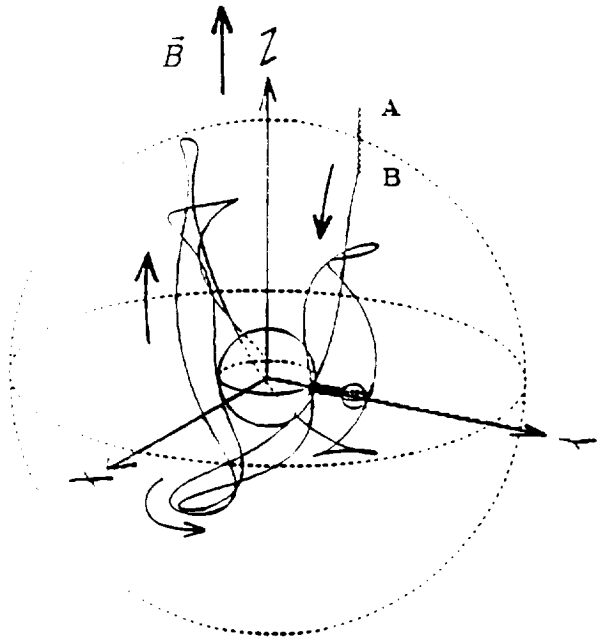

(a) 3-D view

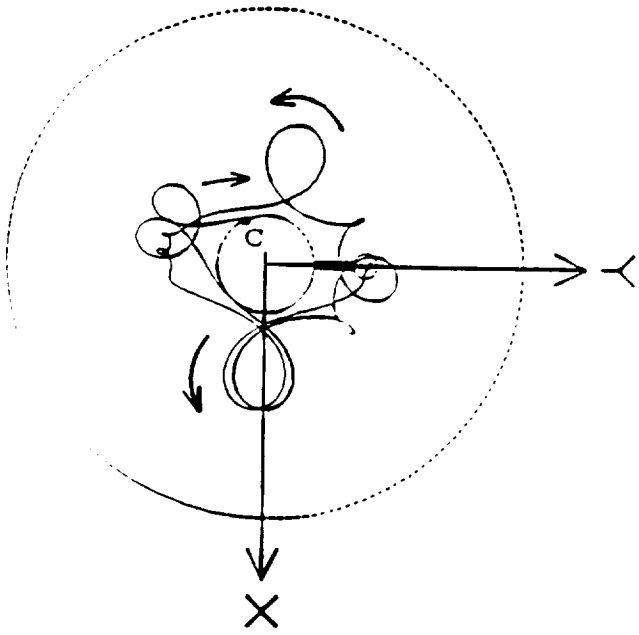

(b) Top view

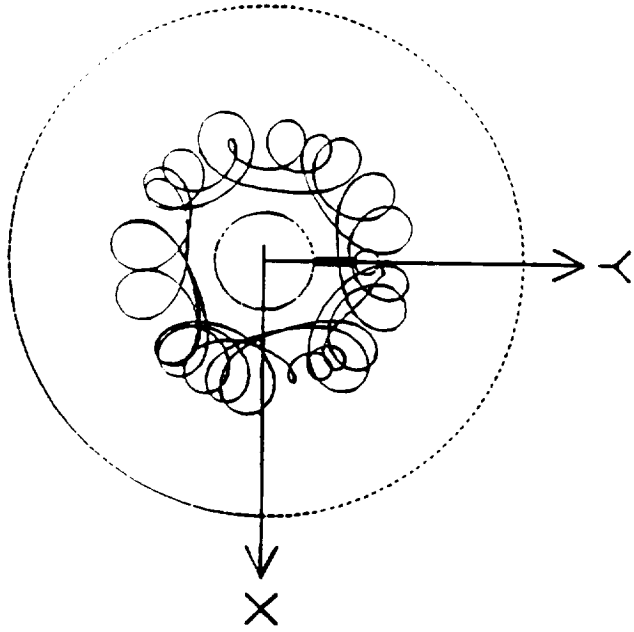
Y
X

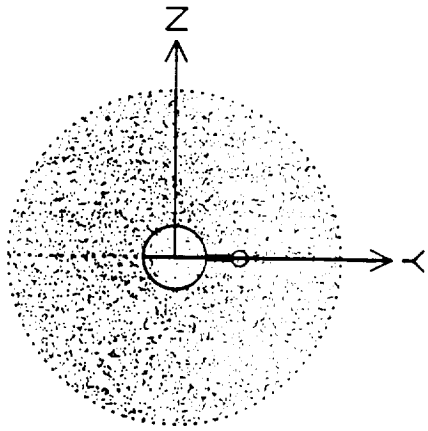

(a) Time = 0.000 $2\pi/\omega_p$

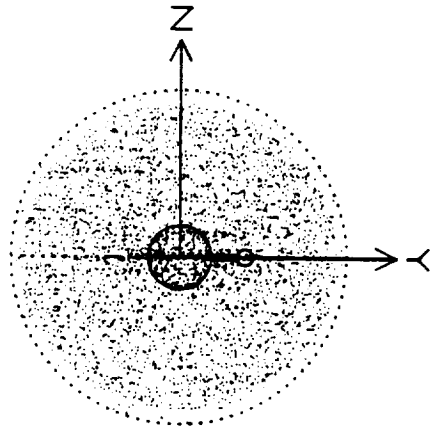

(b) Time = 1.423 $2\pi/\omega_p$

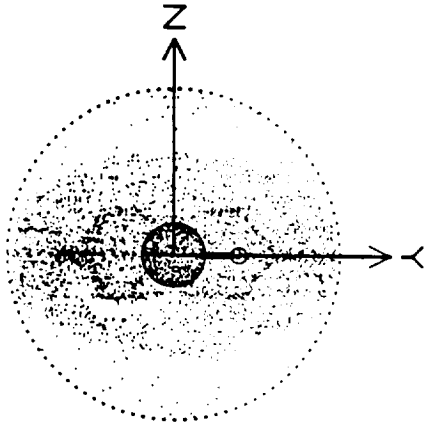

(c) Time = 2.846 $2\pi/\omega_p$

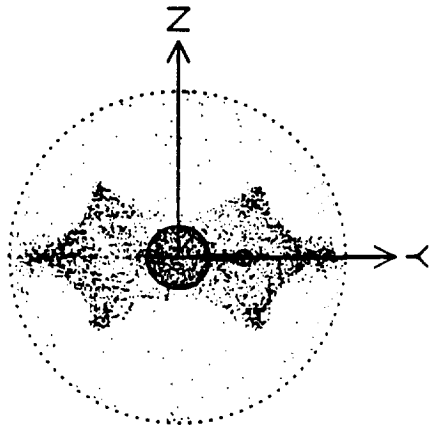

(d) Time = 4.269 $2\pi/\omega_p$

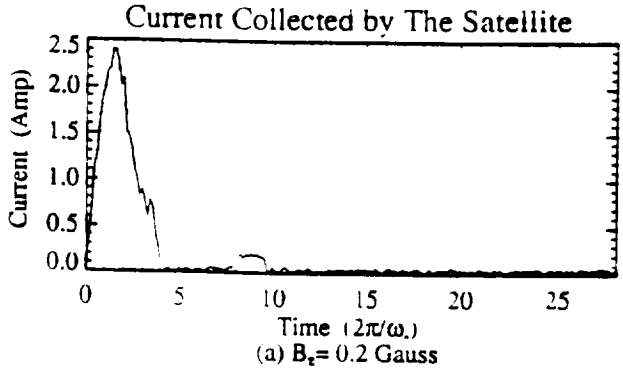

(a) B_z= 0.2 Gauss

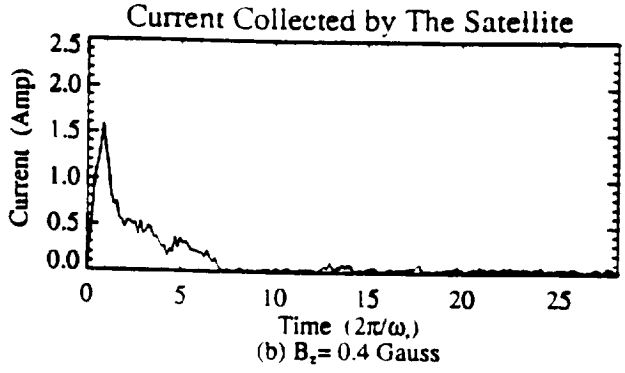

(b) B_z= 0.4 Gauss

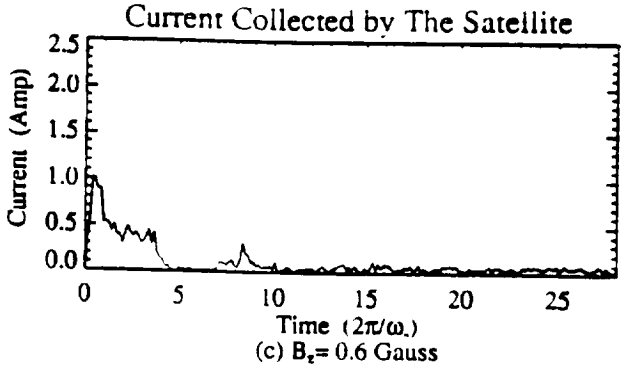

(c) B_z= 0.6 Gauss

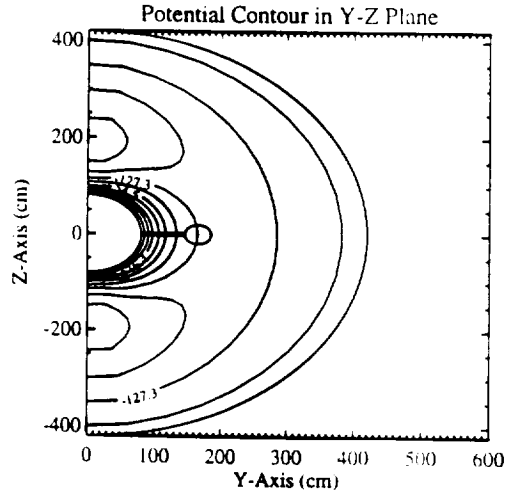
Potential Contour in Y-Z Plane
400
200
0
-200
-400
Z-Axis (cm)
0
100
200
300
400
500
600
Y-Axis (cm)

(a)

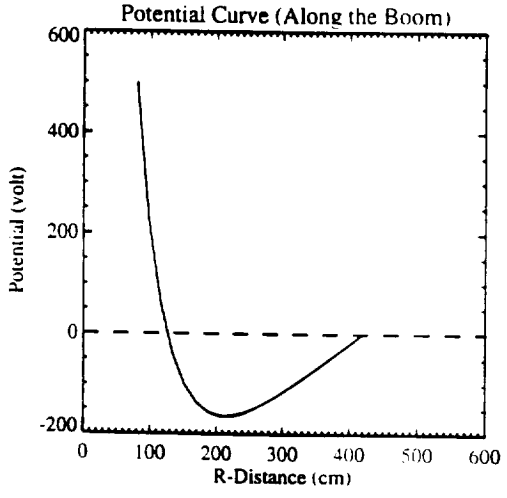
Potential Curve (Along the Boom)
600
400
200
0
-200
Potential (volt)
0
100
200
300
400
500
600
R-Distance (cm)

(b)

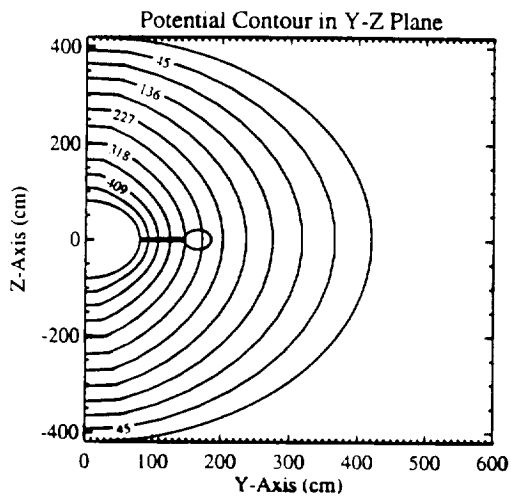
Potential Contour in Y-Z Plane
400
200
0
-200
-400
Z-Axis (cm)
45
136
227
318
409
0
100
200
300
400
500
600
Y-Axis (cm)

(c)

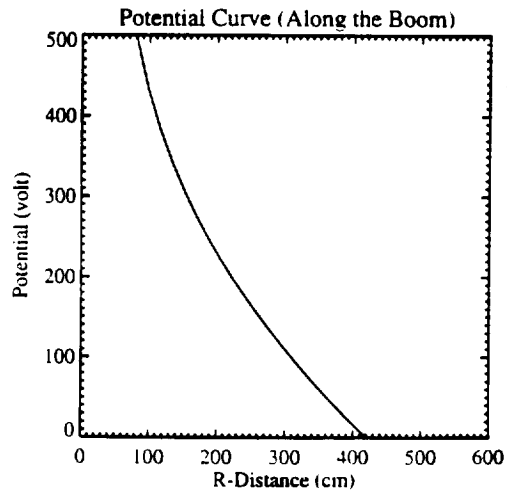
Potential Curve (Along the Boom)
500
400
300
200
100
0
Potential (volt)
0
100
200
300
400
500
600
R-Distance (cm)

(d)

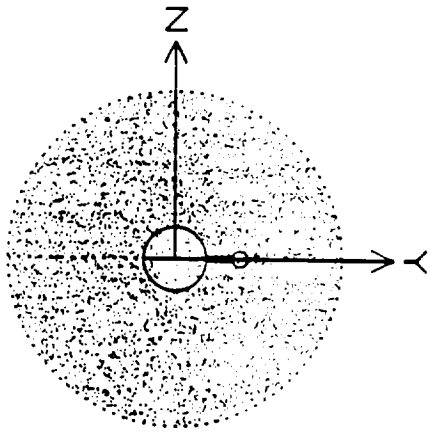

(a) **Time = 0.000** $2\pi/\omega_p$

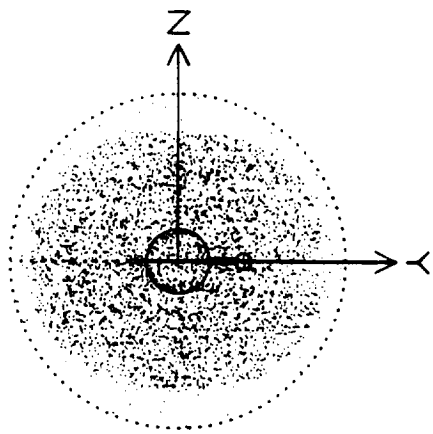

(b) **Time = 1.423** $2\pi/\omega_p$

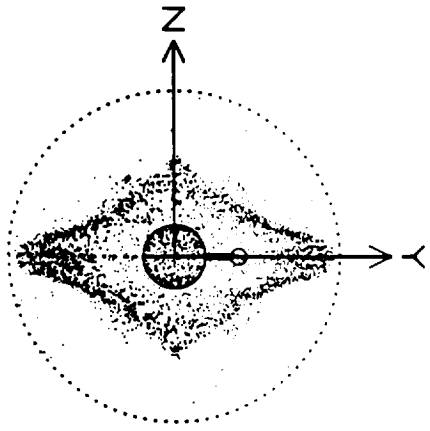

(c) **Time = 2.846** $2\pi/\omega_p$

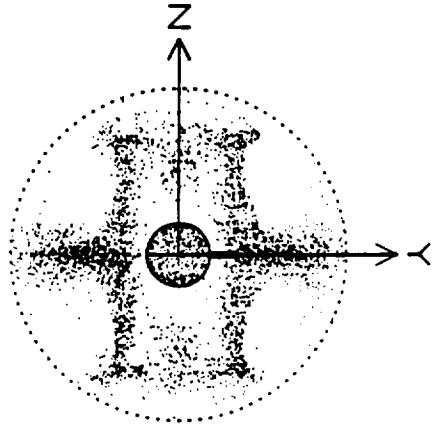

(d) **Time = 4.269** $2\pi/\omega_p$

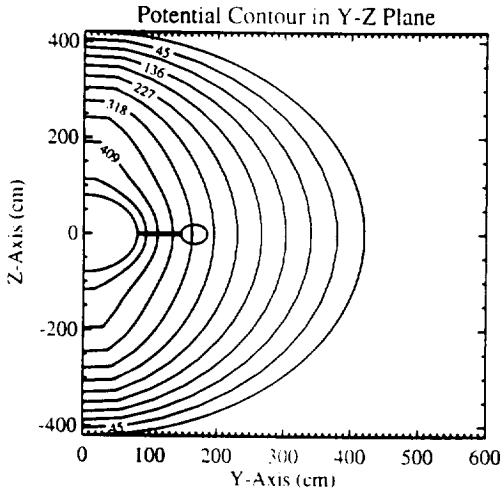
Potential Contour in Y-Z Plane
400
200
0
-200
-400
45
136
227
318
409
45
Z-Axis (cm)
0
100
200
300
400
500
600
Y-Axis (cm)

(a)

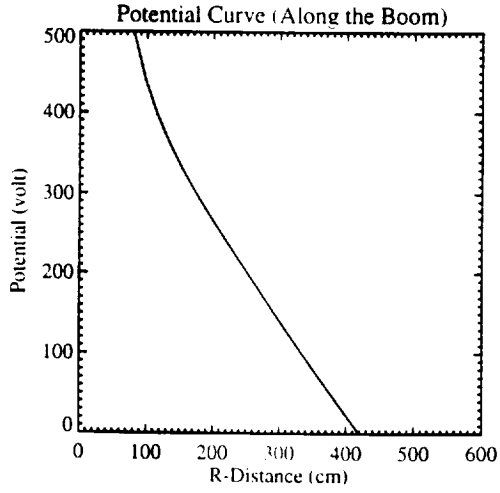
Potential Curve (Along the Boom)
500
400
300
200
100
0
Potential (volt)
0
100
200
300
400
500
600
R-Distance (cm)

(b)

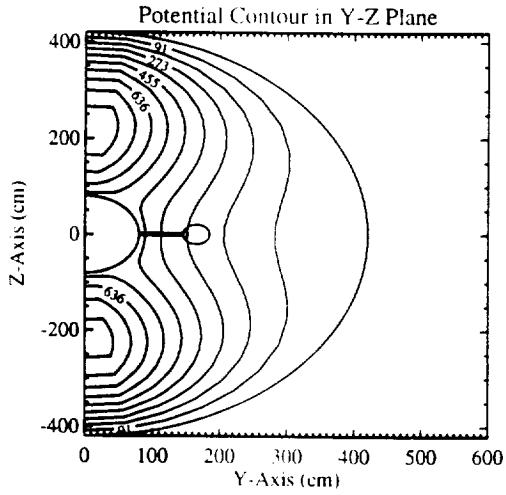
Potential Contour in Y-Z Plane
400
200
0
-200
-400
Z-Axis (cm)
91
273
455
636
636
91
0
100
200
300
400
500
600
Y-Axis (cm)

(a)

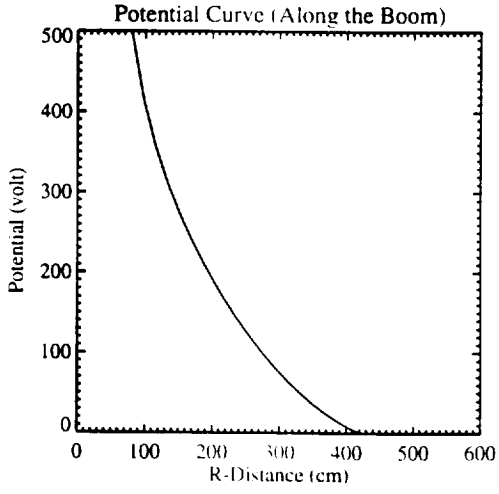
Potential Curve (Along the Boom)
500
400
300
200
100
0
Potential (volt)
0
100
200
300
400
500
600
R-Distance (cm)

(b)

Fig 11

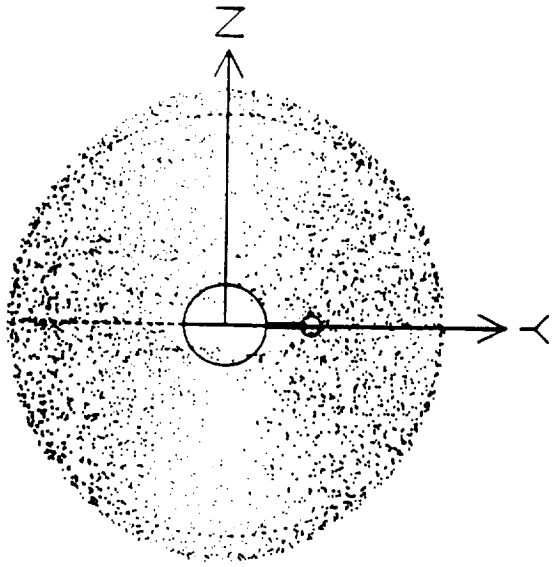
Z
Y

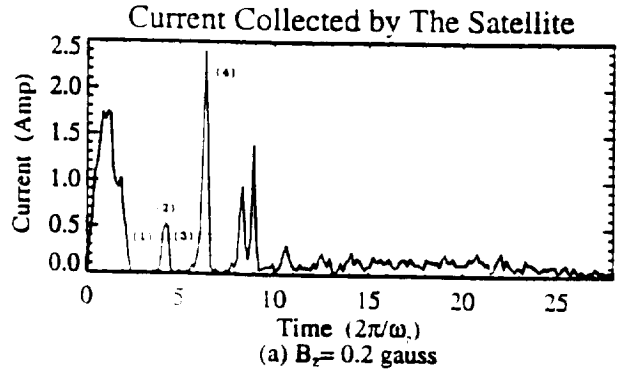

(a) B_z= 0.2 gauss

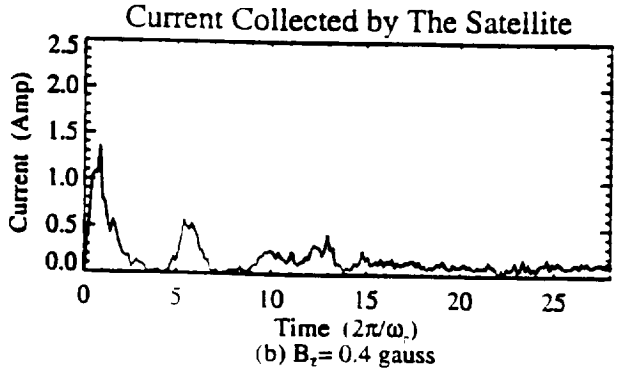

(b) B_z= 0.4 gauss

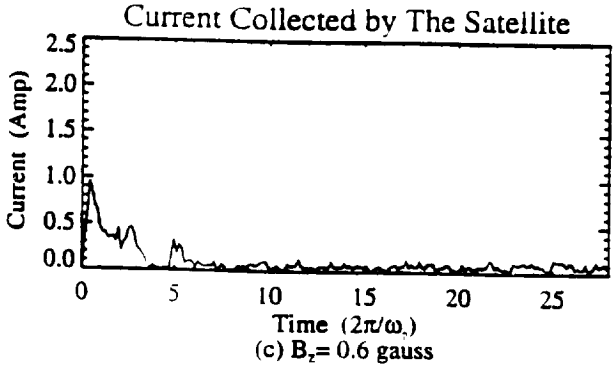

(c) B_z= 0.6 gauss

Fig 13

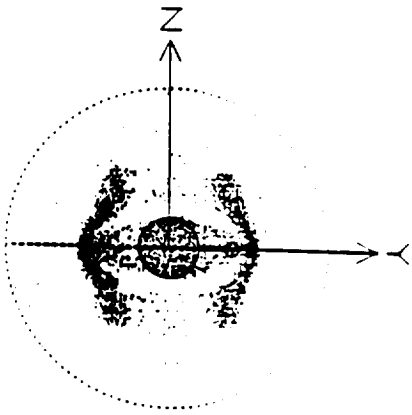

(a) Time = 2.561 $2\pi/\omega_p$

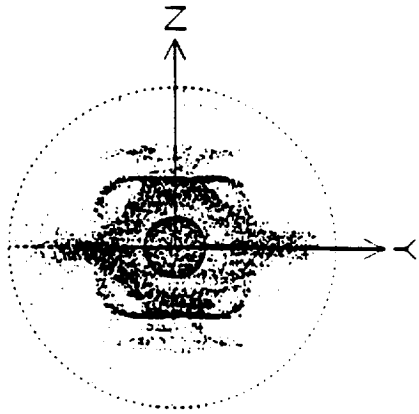

(b) Time = 4.269 $2\pi/\omega_p$

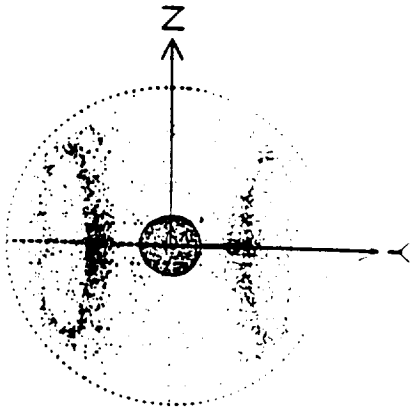

(c) Time = 5.123 $2\pi/\omega_p$

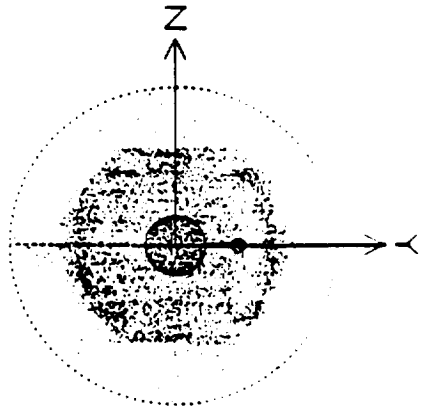

(d) Time = 6.261 $2\pi/\omega_p$

DOC #: 24943 ABSTRACT SCREEN PAGE: 1 ** WORDS NOT FOUND *

Research on Orbital Plasma-Electrodynamics (ROPE)

ABQ: NC
ABA: Author (revised)

CIN: SAF
KIN: JXP
AIN:

Since the development of probe theory by Langmuir and Blodgett, the problem of current collection by a charged spherically or cylindrically symmetric body has been investigated by a number of authors. This paper overviews the development of a fully three-dimensional particle simulation code which can be used to understand the physics of current collection in three dimensions and can be used to analyze data resulting from the future tethered satellite system (TSS) According to the TSS configurations, two types of particle simulation models were constructed: a simple particle simulation (SIPS) and a super particle simulation (SUPS). The models study the electron transient response and its asymptotic behavior around a three dimensional, highly biased satellite. The potential distribution surrounding the satellite is determined by solving Laplace's equation in the SIPS model and by solving Poisson's equation in the SUPS model.

SIPS
SUPS
SIPS
SUPS

PF1=ABA LIST; PF2=RESET; PF3=SIGNON; PF4=RELEASE FROM SUBQ; PF5=SELECTION;
PF6=SUBQUEUE; PF7=STORE ABSTRACT; PF8=MAI; PF10=SEND TO 'MAIQ';
PF14=PREVIOUS PAGE; PF15=NEXT PAGE; PF19=TITLE-EXT; PF20=INDEX TERMS

4B• X () A =-•PC LINE 11 COL 2

Research on Orbital Plasma-Electrodynamics (ROPE)

ABQ: NC
ABA: Author (revised)

CIN: SAF
KIN: JXP
AIN:

Thus, the potential distribution in space is independent of the density distribution of the particles in the SUPS model but it does depend on the density distribution of the particles in the SUPS model. The evolution of the potential distribution in the SUPS model is described. When the spherical satellite is charged to a highly positive potential and immersed in a plasma with a uniform magnetic field, the formation of an electron torus in the equatorial plane (the plane in perpendicular to the magnetic field) and elongation of the torus along the magnetic field are found in both the SIPS and the SUPS models but the shape of the torus is different. The areas of high potential that exist in the polar regions in the SUPS model exaggerate the elongation of the electron torus along the magnetic field.	SUPS SUPS SUPS SIPS/SUPS SUPS/EXAGGERATE

DOC #: 24943 ABSTRACT SCREEN PAGE: 3 ** WORDS NOT FOUND *

Research on Orbital Plasma-Electrodynamics (ROPE)

ABQ: NC
ABA: Author (revised)

CIN: SAF
KIN: JXP
AIN:

The current collected by the satellite for different magentic field strengths is investigated in both models. Due to the nonlinear effects present in SUPS, the oscillating phenomenon of the current collection curve during the first 10 plasma periods can be seen (this does not appear in SIPS). From the parametric studies, it appears that the oscillating phenomenon of the current collection curve occurs only when the magnetic field strength is less than 0.2 gauss for the present model.

SUPS

SIPS

PF1=ABA LIST; PF2=RESET; PF3=SIGNON; PF4=RELEASE FROM SUBQ; PF5=SELECTION;
PF6=SUBQUEUE; PF7=STORE ABSTRACT; PF8=MAI; PF10=SEND TO 'MAIQ';
PF14=PREVIOUS PAGE; PF15=NEXT PAGE; PF19=TITLE-EXT; PF20=INDEX TERMS

4B• A =-•PC LINE 11 COL 2

DOC NUMBER: 24943 INDEXING: SUBJECT/TERMS SCREEN CIN: SAF
TITLE: Research on Orbital Plasma-Electrodynamics (ROPE) KIN: JXP
AIN:

	MAJOR TERMS:	SWITCH
1:	PLASMA ELECTRODES	_
2:	COMPUTERIZED SIMULATION	_
3:	TETHERED SATELLITES	_
4:	MATHEMATICAL MODELS	_
5:	POISSON EQUATION	_
6:	MAGNETIC FIELDS	_
7:	TORUSES	_
8:	PLASMA PROBES	_
9:	CURRENT SHEETS	_
10:		_
11:		_
12:		_
13:		_
14:		_
15:		_

	MINOR TERMS:	
1:	POLAR REGIONS	_
2:	PLASMA DYNAMICS	_
3:	TRANSIENT RESPONSE	_
4:	DENSITY DISTRIBUTION	_
5:	THREE DIMENSIONAL MODELS	_
6:	ASYMPTOTIC PROPERTIES	_
7:		_
8:		_
9:		_
10:		_
11:		_
12:		_
13:		_
14:		_
15:		_

PROPOSED TERMS:

PF2=RESET; PF3=SIGNON; PF4=RELEASE; PF5=SELECTION; PF6=SUBQ
PF10=ALPHA; PF11=HIERARCHY; PF12=STORE; PF13=CENTRAL SCREEN; PF20=TITLE/WNF
4B• A =-•PC LINE 21 COL 11